WCTE 2016
World Conference on Timber Engineering
August 22-25, 2016 | Vienna, Austria

NUMERICAL SIMULATIONS OF TIMBER CONNECTIONS WITH ANGLE BRACKETS SUBJECTED TO EXTERNAL LOADING

Petr Sejkot[1], Petr Kuklík[2], Sigurdur Ormarsson[3], Panagiotis Patlakas[4], Robert Jára[5], Jan Pošta[6]

ABSTRACT: The paper presents experimental, numerical, and analytical methods for the prediction of the load-bearing capacity of timber connections with metal angle brackets, utilising annular ring nails as fasteners. Full-scale testing experiments were performed in order to obtain the stiffness of the connection. Numerical simulations are employed to predict the load-bearing capacity of the angle brackets, when the external force is in the direction of the opening of the angle bracket. The characteristic load-bearing capacity of the connection was calculated using both the results of the numerical simulation, and analytical formulas, utilising laboratory measurements of the timber density. The paper presents the results of the three approaches, allowing direct comparison of the veracity of the simulations.

KEYWORDS: Timber structures, spatial nailing plates, joints with fitting, annular ring nails, numerical simulations

1 INTRODUCTION

This paper presents an analysis of connections of timber members with angle brackets, using annular ring nails subjected to external loading. The analysis was made experimentally, numerically, and analytically.

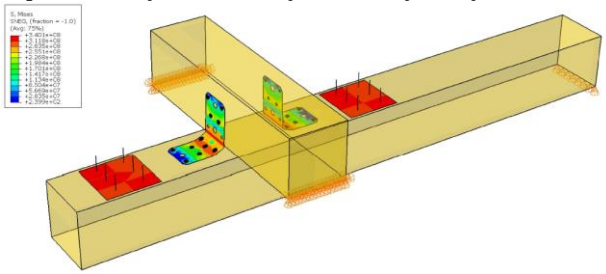

Figure 1: *Geometry and boundary conditions of the test set-up studied.*

The investigated connection (Figure 1) belongs to the category of spatial connections with thin-walled metal elements which are gradually supplanting traditional carpentry joints. Their principal advantage is that they do not significantly weaken the connected timber members. Other advantages include the possibility of easy in-situ constructability or the possibility of direct connection of timber members to steel and concrete structural systems.

[1] Petr Sejkot, Czech Technical University in Prague, UCEEB Trinecka 1024, 273 43 Bustehrad, Czech Republic, petr.sejkot@cvut.cz
[2] Petr Kuklík, CTU in Prague, Czech. Rep., kuklik@fsv.cvut.cz
[3] Sigurdur Ormarsson, LNU, SWE, sigurdur.ormarsson@lnu.se
[4] Panagiotis Patlakas, Southampton Solent University, UK, panagiotis.patlakas@solent.ac.uk
[5] Robert Jára, CTU in Prague, Czech. Rep., robert.jara@cvut.cz
[6] Jan Pošta, CTU in Prague, Czech. Rep., jan.posta@uceeb.cz

Another important advantage is their ductile behaviour when subjected to loading [1].
The most common type of a thin-walled metal connection consists of an steel angle bracket fastened to the timber members with annular ring nails (Figure 2).

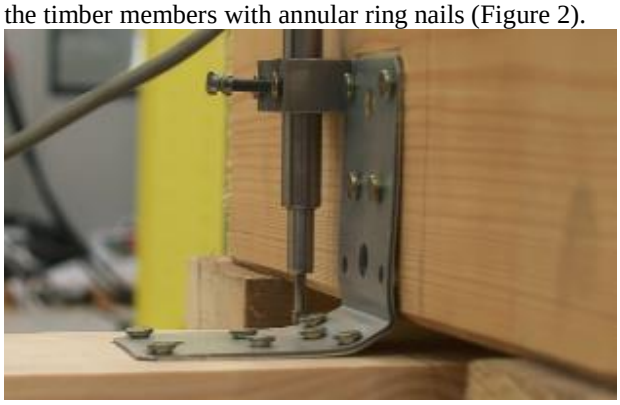

Figure 2: *Steel angle bracket spatial joint during the load-bearing test.*

Their main disadvantage is a very complex behaviour when subjected to loading. Connections using angle brackets are often loaded from various directions. The load distribution to the nails is not uniform and is not easily predictable due to the f high ductility of the metal plates. Moreover, deformed metal plates also cause prying of nails, i.e. loading them by an additional bending moment. Currently there is no standardized calculation procedure to determine their load bearing capacity and such connections are typically designed according to the manufacturers' experiment-based results.
This creates obvious limitations for designers, restricting their capacity to check such connections with simplified analytical models. Thus the development of reliable

calculation models would have concrete benefits both for manufacturers (faster and cheaper product development) and designers (increased confidence in their use).
A commonly accepted method for the analysis of steel-to-timber connections is 3D Finite Element Analysis (FEA), as described in [2]. This was used in the development of the shape of a new angle bracket, produced by the Czech manufacturer BOVA Březnice, which significantly improves its load bearing capacity without an increase in cost (Figure 3).

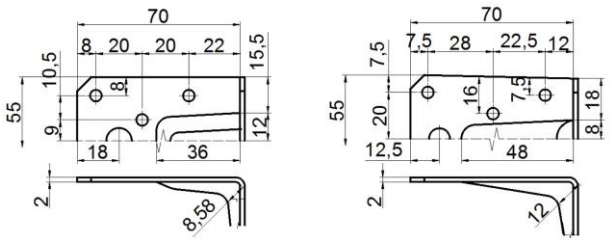

Figure 3: *Left – original, right – improved version of angle bracket with a rib (dimensions in millimetres).*

Both the load-bearing capacity and the stiffness of the connection were higher with the use of this improved angle brackets; this was predicted by FEA simulations and validated by full-scale experiments (Figure 4).

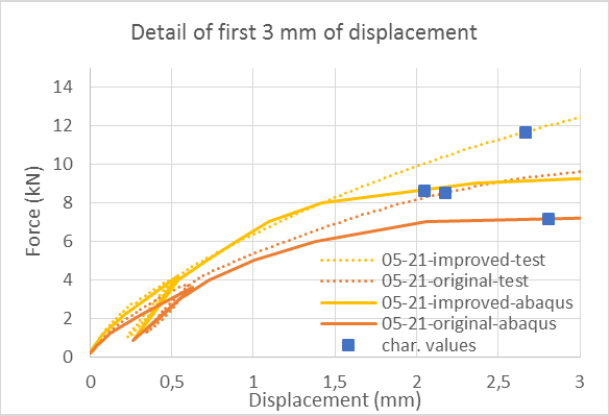

Figure 4: *Results from numerical simulations compared to full-scale tests data. Force-displacement curves represent the opening of the gap between the beams connected by two different versions of angle brackets with a rib under the applied external load [2].*

The improvement in stiffness is evident when the load bearing capacities at a displacement of 3 mm are compared (Table 1). The value was chosen as practising engineers need to know the behaviour of a connection not only in the Ultimate Limit State (where deformations can exceed 10 mm) but also in the Serviceability Limit State (SLS).

Table 1: *Ultimate (max) and Serviceability Limit State (3 mm) - characteristic load-bearing capacities*

	Original rib	Improved rib
Experiments (max):	8,50 kN	11,67 kN
Experiments (3 mm):	7,01 kN	10,41 kN
Numerical (max):	7,15 kN	8,63 kN
Numerical (3 mm):	5,98 kN	7,21 kN

Despite the undeniable benefits of FEA models and full-scale experiments, there is still a demand for analytical calculation models of connections using thin-walled metal elements, especially by practising engineers. As such, an analytical model was developed at the University Centre for Energy Efficient Buildings (part of the Czech Technical University in Prague). This model is presented in this paper and its results are compared to results obtained from FEA simulations and full-scale experiments.

2 FULL-SCALE EXPERIMENTS

The experiments (see Figure 5) were performed according to EOTA TR 16 [3].

Figure 5: *Joint during load-bearing test.*

The tested connections were loaded following the loading diagram in Figure 6, which is based on the expected load-bearing capacity of the tested angle brackets.

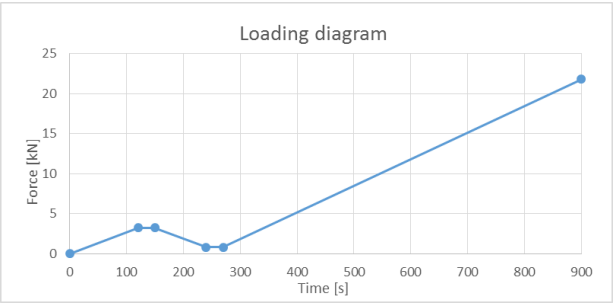

Figure 6: *Loading diagram of the tested samples*

In the first 120 seconds of the test, the connection was loaded to 40% of its expected load bearing capacity and

left in that state for 30 seconds. Then, in 90 seconds the connection was uniformly unloaded to 10% of the expected load-bearing capacity and left in that state for 30 seconds. Finally, it was loaded to failure at a rate of 3.33% of the expected load-bearing capacity per second.
Partial load bearing capacities were determined by two limits – collapse and maximum displacement of 15 mm. The force was applied by a hydraulic cylinder with a preset loading program in time.
The displacement was measured by a group of sensors. All input data were synchronised in the measuring centre.

2.1 EXPERIMENTAL SET-UP AND EVALUATION OF RESULTS

The full-scale experiment consists of two timber (spruce) beams 100 x 100 mm in cross section, 400 mm and 1010 mm long. Beams are connected by two BV/U angle brackets 55x70x70 mm (BOVA Březnice, type 05-21). Each angle bracket is connected to the beam by 11 annular ring nails 4.0/60 mm (7 in the horizontal branch of the angle bracket and 4 in the vertical branch).

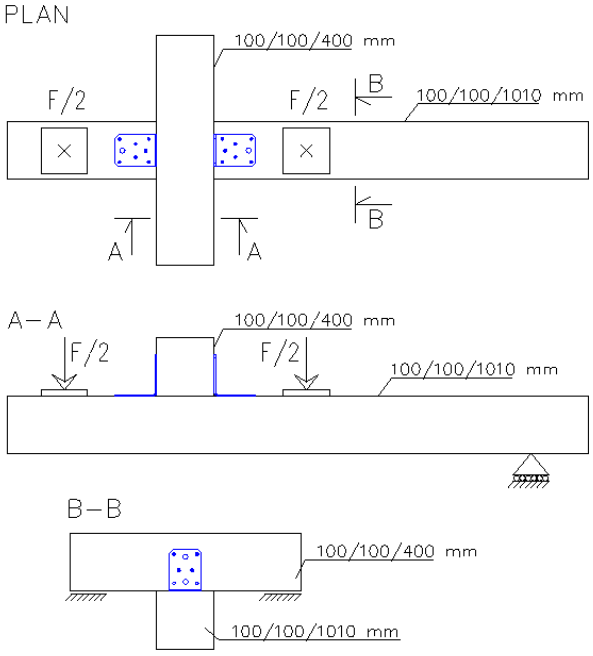

Figure 7: *Test set-up.*

To achieve the load opening the joint, shorter upper beam was supported on both sides and longer lower beam was supported only on one side (see Figure 7). Although in this set-up both angle brackets were not loaded equally, the difference was so minor that it could be neglected in the analytical calculation approach.
Experiments were performed at the University Centre for Energy Efficient Buildings in Buštěhrad (Figure 5), which is part of the Czech Technical University in Prague. To avoid displacement sensors destruction, they were removed when reaching 12 mm, after which only the maximum force before the connection destruction was measured. The dimensions of the angle brackets (see Figure 8) were designed according to approach presented in [2].

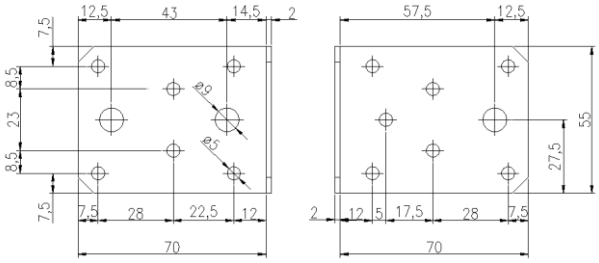

Figure 8: *Angle bracket dimensions in millimetres (left – vertical part, right – horizontal part).*

2.1.1 Evaluation of measured densities

The characteristic value of mass density (an input into the fastener load bearing capacity calculation) was determined as α-percentile in the normally distributed function according to Eurocode 0 [4].
The possibility to relate the results of the tests to the appropriate timber class [5] was checked according to ISO 8970 [6], i.e.:

$$0.95 \cdot \rho_m \le \rho_{m,sel} \le 1.05 \cdot \rho_m \qquad (1)$$

$$(1-k)\rho_m \le \rho \le (1+k)\rho_m \qquad (2)$$

where ρ_m the mean value of appropriate timber class density,

$\rho_{m,sel}$ the measured mean value of timber density of tested specimens,

ρ the measured density of each tested specimen,

$k = 1{,}6\ \sigma/\rho_m$, where σ is the standard deviation of density of the appropriate timber class (i.e. difference between mean and characteristic density divided by value 1,64485 which is 95 % quantile derived from distribution function of standard normal distribution).

If condition (2) is not satisfied and specimens are used to determine the characteristic value of the load bearing capacity of timber connections using fitting, values from tests cannot be used directly and must be modified.

2.1.2 Evaluation of measured connection load-bearing capacities

The modification of the measured load-bearing capacities should be used not only for the case when condition (2) is not fulfilled but also for application of results obtained from tests using one timber strength class to get characteristic load-bearing capacity in another timber strength class and should be made as follows:

$$F_{\max,\mathrm{mod}} = F_{\max} \cdot \left(\rho_{\mathrm{mean}} / \rho\right) \qquad (3)$$

where: $F_{max.mod}$ the modified load bearing capacity of the connection

F_{max} the measured load bearing capacity of the connection,

ρ_{mean} the mean value of timber density to which results are related

ρ the measured timber density of tested connection.

It is also convenient to transform measured load-bearing capacities of tested connection to dimensionless value by a coefficient:

$$C_{LN} = \exp\left(1 - \frac{1}{n} \cdot \sum_{i=1}^{n} \ln(m_i)\right) \quad (4)$$

where n number of measured load-bearing capacities,

m_i measured load-bearing capacities modified to appropriate timber class.

Thanks to the transformation (4), the mean value of this logarithmically normally distributed function is equal to one.

$$\bar{y} = \frac{1}{n}\sum_{i=1}^{n} \ln(m_i \cdot C_{LN}) = 1.000 \quad (5)$$

where: n number of test values in the sample

m_i partial measured values.

Due to the fact that the measured standard deviation of the wood density is very often lower than the standard deviation of appropriate timber class, it should be checked that it is fulfilled the condition:

$$\left(\sqrt{\frac{1}{n-1}\sum_{i=1}^{n}(\ln m_i \cdot C_{LN} - \bar{y})^2}\right) \geq 0.1 \quad (6)$$

If modification (3) of the measured load-bearing capacities is not used, the coefficient of variation of the load-bearing capacity considering full variation of the wood density is calculated as:

$$COV_R^2 = (COV_\delta^2 + 1)\left(\frac{c_p \cdot 0.1^2 + 1}{c_p \cdot COV_\rho^2 + 1}\right) - 1 \quad (7)$$

If modification (3) is used for the measured load-bearing capacities, the coefficient of variation of the load-bearing capacity considering full variation of the wood density is calculated as:

$$COV_R^2 = (COV_\delta^2 + 1)(c_p \cdot 0.1^2 + 1) - 1 \quad (8)$$

where c_p depends on the fastener type and the course of reduction; in this case a value 1.0 is used, because fasteners belong to the threaded nails category and the reduction is always from a higher to lower density.

The coefficient of variation of the measured wood density used in (7) and (8) is:

$$COV_\rho = \frac{\sqrt{\frac{1}{n-1}\sum_{i=1}^{n}(m_i - \left(\frac{1}{n}\sum_{i=1}^{n} m_i\right))^2}}{\frac{1}{n}\sum_{i=1}^{n} m_i} \quad (9)$$

where n the number of measured timber densities,

m_i the measured timber densities.

The coefficient of variation of the measured load-carrying capacity used in (7) and (8) is:

$$COV_\delta = \frac{\sqrt{\frac{1}{n-1}\sum_{i=1}^{n}\left(\ln m_i - \frac{1}{n}\sum_{i=1}^{n}\ln(m_i)\right)^2}}{\frac{1}{n}\sum_{i=1}^{n}\ln(m_i)} \quad (10)$$

where n the number of measured load-bearing capacities,

m_i the measured load-bearing capacities modified to the appropriate timber class and transformed by C_{LN} according to (4).

All the coefficients of variation are then taken into account by a factor that increases the standard deviation of the load-carrying capacity:

$$k_{\mathrm{cov}} = COV_R / COV_\delta \quad (11)$$

This factor reduces the standard deviation of the measured load-bearing capacities to:

$$s_y = \max\left(k_{\mathrm{cov}}\sqrt{\frac{1}{n-1}\sum_{i=1}^{n}(\ln m_i - \bar{y})^2}; 0.05\right) \quad (12)$$

The characteristic load-bearing capacity of the tested connections was calculated as:

$$F_{ax,Rk} = \exp\left(\bar{y} - \frac{6{,}5 \cdot n + 6}{3{,}7 \cdot n - 3} \cdot s_y\right) \cdot C_{LN} \quad (13)$$

where n the number of measured load-bearing capacities,

$\bar{y}$ their mean value calculated according to (5),

s_y their standard deviation calculated according to (12) and coefficient C_{LN} is calculated according to (4).

2.2 EXPERIMENTALLY OBTAINED RESULTS

In all tested joints the dependence between the value of the external force and the gap between the connected beams was measured. The plot shows (Figure 9) the tested connections exhibit significantly plastic behaviour.

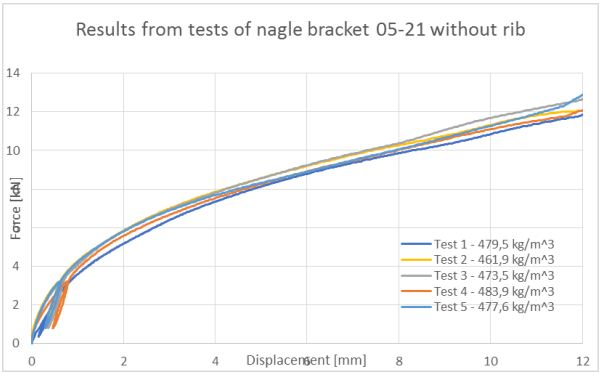

Figure 9: *Displacement to force diagram of gap between connected beams development for each tested connection.*

There is also remarkably good conformity between all the measured behaviours that indicates that the steel angle bracket achieves ultimate strength before the nails start to be pulled out.
The experimentally determined load-bearing capacities of the connections were compared to the results from numerical simulations and analytical solutions.
Measured densities of tested angle brackets are presented in Table 2.

Table 2: *Evaluation of measured density*

Angle bracket 05-21	No rib
Number of specimens	5
Mean density	475.3 kg/m^3
Standard deviation	23.8 kg/m^3
Characteristic density	419,9 kg/m^3

Compared to the density values found in EN 338 [5] for timber strength classes using condition (1) for mean density, it is obvious that the timber members of the tested connections can be classified as C30, as their mean densities are between 437 kg/m^3 and 483 kg/m^3. However, the used nails were tested in timber class C24 and therefore it is necessary to modify the measured load-bearing capacities of the connection using (3).

Table 3: *Consideration of the natural variation of wood density with respect to the measured load-carrying capacities in evaluation of measured load bearing capacities.*

Angle bracket 05-21	No rib
Mean capacity (measured in C30):	13.00 kN
Mean capacity (modified to C24):	11.49 kN
COV_ρ (9):	1.76 %
COV_δ (10):	5.38 %
Used values:	Modified
COV_R (8):	11.23 %
k_{cov} (11):	2.09
Characteristic capacity (in C24):	8.69 kN

Nevertheless, it is important to point-out that these load-bearing capacities are related to the collapse of the connection after deformation more than 10 millimetres. If SLS is decisive, and thus the maximum allowable deformation value is 3 mm, the characteristic load-bearing capacity of whole connection would be only 4.68 kN.

3 ANALYTICAL MODEL

Analytical calculations determining load-bearing capacities of tested angle brackets were inspired by a research project at the University of Trento [7]. Branches of angle brackets are simplified to beams. Fasteners are simplified to springs. The end of the horizontal branch of each angle bracket and the abutment of the vertical branch is leaning against the timber of the lower beam (Figure 10).

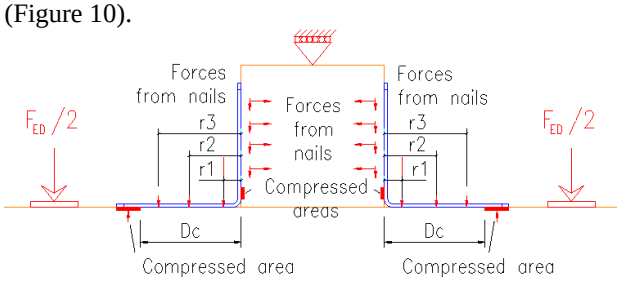

Figure 10: *Analytical static model*

Load distribution to the individual nails is linear and given by the length of the compressed area at the end of horizontal branch of the angle bracket. Simultaneously, it must fulfil the maximum bending moment condition. The length of the compressed area at the end of the angle bracket was determined by a parametric study.
The axial withdrawal capacity of the annular ring nail fasteners was calculated according to Eurocode 5 [8], utilising the characteristic pointside withdrawal strength provided by the manufacturer, HAŠPL [9].
The parametric study was performed in SMATH Studio [10]. This study started with 1 mm long part of horizontal branch of the angle bracket compressed to the timber. It is assumed that this part is behind the plastic hinge which bends the branch of the angle bracket and induces force acting against the forces in pulled-uot nails (Figure 11).

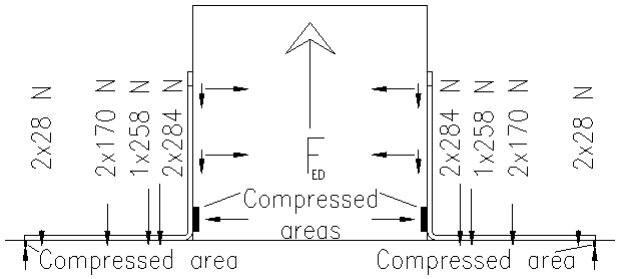

Figure 11: *Load-bearing capacity at the first step of the parametric study.*

This first step determined the maximum load in the whole connection, equal to 2,078 kN. After that, the maximum bending moment in the corner of the angle bracket was reached.
Figure 12 shows the check of the bending moment at the horizontal branch of the angle bracket. Upper and lower

red dots represent minimum and maximum allowed bending moment in the checked cross-sections. Intermediate green dots represent the calculated values of the bending moment in the checked cross-sections.

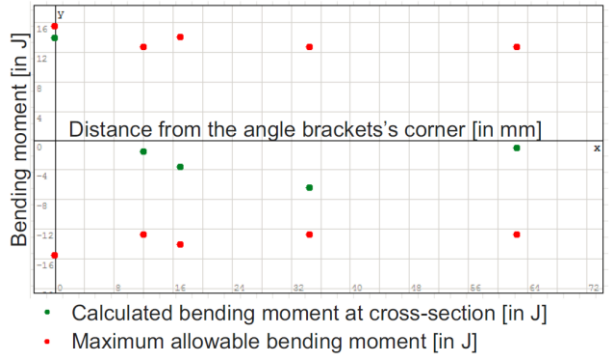

Figure 12: *Bending moment graphical check at the horizontal branch of the angle bracket at the first step of the parametric study.*

The cross-sections were chosen to be checked in places with expected local extremes of bending moments. These are the corner of the angle bracket and points where angle brackets are nailed to beams (see Figure 1 Figure 13).

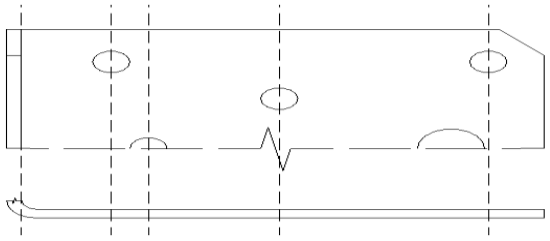

Figure 13: *Cross-sections checked in the analytical model*

In the next step, the part of horizontal branch of the angle bracket compressed to the timber was increased by 1 mm to 2 mm and maximum load in the whole connection was determined again by the same way.
This procedure was made for each milimeter. The highest load-bearing capacity was found when compressed part of the angle bracket horizontal branch was 53 mm long.

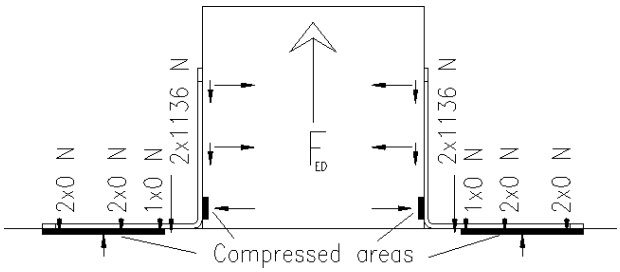

Figure 14: *Load-bearing capacity at the last step of the parametric study.*

This step determined the maximum load in the whole connection, equal to 3,963 kN. After that, the maximum bending moment in the corner of the angle bracket was reached.
Figure 15 shows the check of the bending moment at the horizontal branch of the angle bracket. Upper and lower red dots represent minimal and maximum allowed bending moment in the checked cross-section. Intermediate green dot represents calculated value of the bending moment in the checked cross-section.

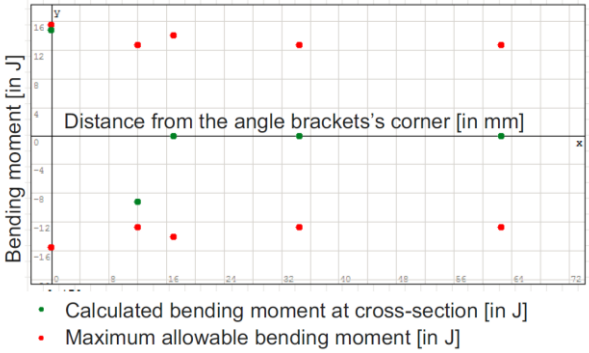

Figure 15: *Bending moment graphical check at the horizontal branch of the angle bracket at the last step of the parametric study.*

Although the calculated load-bearing capacity of whole connection equal is quite conservative, it fulfils SLS criteria (deformation lower than 3 mm), typically required by practitioners.
For validation purposes, this analytic model was also applied to the experimental results obtained in [2]. Results are presented in Table 4.

Table 4: *Characteristic load-bearing capacity*

Calculated characteristic load-bearing capacity	
No rib	3,96 kN
Original rib	4.04 kN
Improved rib	8,07 kN

4 FEA MODEL

The test set up used to determine the load bearing capacities of beam-to-beam connections made by nailed angle brackets has been simulated with a 3D-model in Abaqus CAE [11] (Figure 1). This aims to compare the numerical results with the experimental behaviour presented in this paper. Boundary conditions in the simulation were set according to the real test set-up: the pinned end of the longer shoulder of the lower beam and both ends of the upper beam. In the experiment, the connection was loaded using a load distribution device symmetrically transferring the external loading force to the two areas on the lower beam of the connection (marked in Figure 1).
The timber beams were modelled as solid members. The wood material was assumed to be an orthotropic material with the following elastic parameters: E_l=9700 MPa, E_r=400 MPa, E_t=220 MPa, ν_{lr}=0.35, ν_{lt}=0.60, ν_{rt}=0.55, G_{lr}=400 MPa, G_{lt}=250 MPa, G_{rt}=25 MPa used in [12].

Angle brackets were modelled as shell elements with attached thickness. The steel material used was considered as an elastic-plastic material with a yield stress σ_y = 280 MPa.

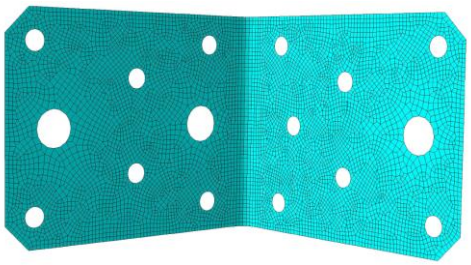

Figure 16: *Element mesh used model for the angle bracket*

The annular ring nails were modelled as connector elements with properties based on the experimental data. However, HAŠPL[9] provides only their load bearing capacities and not the entire stress-strain diagrams. Therefore, complete stress-strain diagrams of used annular ring nails were derived from past experiments (Figure 17), using [13].

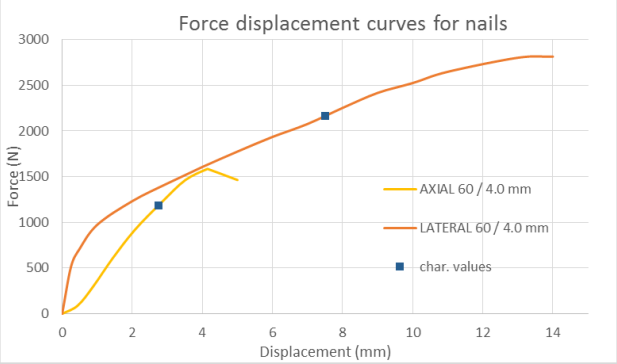

Figure 17: *Force-displacement curves for nails (d=4.0 mm, l = 60 mm) loaded axially and laterally loaded, obtained by experiments.*

Numerical simulations of the beam-to-beam connection brought complete load-displacement curves for the studied connections using angle brackets and predicted its characteristic load-bearing capacity as 6,10 kN in ULS and 4,60 kN in SLS (3 mm displacement). These results were compared to the experimentally determined force-displacement curves. The force represents the external load applied on the connection and displacement is measured considering opening of the gap between the beams in the connection.
Figure 18, shows a comparison between the mean behaviour of the experimentally studied connection and the simulated behaviour of the connection using nail load-bearing capacities calculated considering the measured densities of timber used in the connection set up.

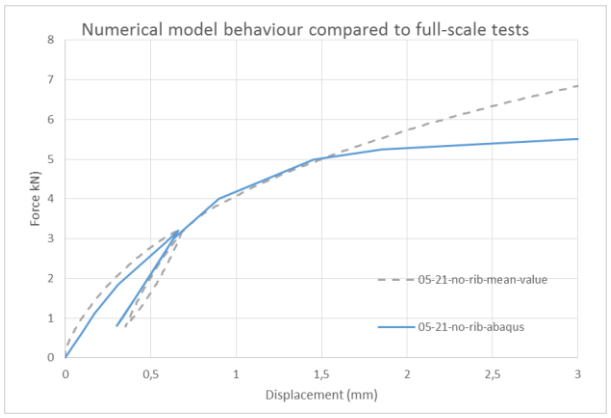

Figure 18: *Results from numerical simulation compared to real behaviour obtained by full-scale tests of the connection*

As is evident from the plot, the simulated curve matches quite well with the experimental curve until it starts to behave nonlinearly (displacement higher than 1.5 mm). This quite high difference between the mean load-bearing capacity of the tested connection and the result from the numerical simulation when it behaves nonlinearly can be explained by omitting the prying of nails. It happens because the angle bracket deformation induces a bending moment in the nails fixed in its holes. This bending moment increases the pressure of the threaded part of the nail on the timber thus increasing its withdrawal resistance.
This behaviour is different to the lateral load, which mainly increases the stress at the smooth part of the nail. This does not increase its withdrawal resistance; conversely, it reduces it due to the rope effect and the plastic motion.
Nevertheless, because of the previously mentioned SLS focus, this research was focused on the behaviour before deformation reached 3 mm.

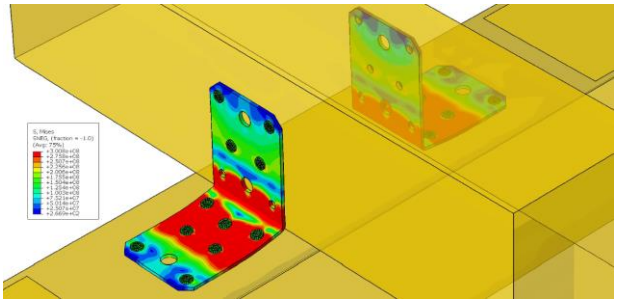

Figure 19: *Contour plot of Von Mises stresses shown on the deformed geometry of the angle brackets in the connection before deformation more than 3 mm occurred.*

After the 3 mm limit, the behaviour of the loaded connections starts to be significantly nonlinear and the deformation is permanent.

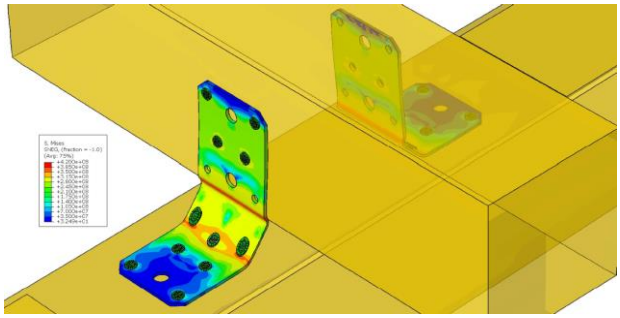

Figure 20: *Contour plot of Von Mises stresses shown on the deformed geometry of the angle brackets in the connection before the collapse when deformation more than 15 mm occurred.*

5 DISCUSSION

In this paper, the stiffness of the numerically modelled connections was compared to data from full-scale tests performed according to the European standards. The simulated load-bearing capacity was compared to analytical calculation based on the European technical reports. Load bearing capacities from the evaluated experiments were compared to the values calculated by analytical methods and by numerical simulations.

Table 5: *Ultimate Limit State - characteristic load-bearing capacity*

Angle bracket 05-21	No rib
Experiments:	8.69 kN
Analytic calculation:	3.96 kN
Numerical simulation:	6,10 kN

It is evident from Table 5, that the analytical approach is much more conservative than the numerical and experimental ones. However when compared with the characteristic load-bearing capacities in the SLS (3mm deformation), the results are much more consistent.

Table 6: *Serviceability Limit State - characteristic load-bearing capacity*

Angle bracket 05-21	No rib
Experiments:	4.68 kN
Analytic calculation:	3.96 kN
Numerical simulation:	4,60 kN

6 CONCLUSIONS

The results presented three approaches for the determination of the load bearing capacities of spatial connections using angle brackets: full-scale experiments according to the European Technical Reports; an analytical method; numerical simulation using simplified material and nail models. All determined load-bearing capacities were listed and compared.

Although the experiments are not dramatically expensive or time consuming, it is useful to have a cheaper, faster and reasonably reliable calculation procedure. The main benefit of the analytical solutions is that they are cheap. However, they are very conservative and their reliability is not well proved.

Numerical simulations provide more applicable results than the analytical solutions. Although numerical modelling of timber is still very challenging and the numerical models employed here were quite simplified, the simulation proved to be a very useful tool for predicting the behaviour of the whole connection and for optimizing the shapes of steel elements in the processed connections. Another considerable advantage of numerical simulations, in comparison to analytical solutions, is that they predict the stiffness of whole connection. When comparing numerical simulations to experimental results, a significant advantage of numerical simulations is the possibility to simulate various loads of the model in various directions which would be quite challenging in laboratory conditions. This is very useful for the design of joints in seismic areas or for special applications such as timber shear walls [7].

It is also interesting to compare results from the research described in this paper to the results of previous work on angle brackets with a rib [2]. The results of the latter [2] were used for the geometry optimization of metal works produced by the Czech company BOVA Březnice (Figure 3).

The comparison of the results of the two projects shows that in connections loaded in this direction, the rib is much more effective than an additional nail in the angle bracket. However angle brackets without a rib have more design flexibility, e.g. in hidden connections.

For further research there is a lot of potential for direct comparing the angle brackets presented in this paper, with hidden plate connections. It is planned to build identical samples with hidden steel-to-timber connections, and test them the exact same way as it was presented in the paper. It will bring very interesting results comparing the two approaches. These connections can be compared also from a construction perspective which means cost buildability.

This like-for-like comparison will find out whether hidden plates perform equally well structurally, and have the fire design advantages (being encases in timber).

ACKNOWLEDGEMENT

This work has been supported by the Ministry of Education, Youth and Sports within National Sustainability Programme I, project No. LO1605.

REFERENCES

[1] Šťastný R.: Tenkostěnné ocelové tvarované elementy používané v dřevařském inženýrství, doctoral thesis CTU in Prague Faculty of Civil Engineering, 2005.

[2] Sejkot, P., Ormarsson, S., Vessby, J., & Kuklík, P.: Determination of load bearing capacity for spatial joint with steel angle brackets. Paper presented at the IOP Conference Series: Materials Science and Engineering, 96(1) doi:10.1088/1757-899X/96/1/012070, 2015.

[3] EOTA TR16: Method of testing - Three-Dimensional Nailing Plates with examples, 2012.
[4] EN 1990 Eurocode 0: Basis of Structural Design Second Edition.
[5] CEN 2003 EN 338: Structural Timber – Strangth Clases.
[6] CEN 2010 EN ISO 8970: Timber Structures – Testing of Joints Made with Mechanical Fasteners – Requirments for Wood Density.
[7] Tomasi R, Sartori T.: Mechanical behaviour of connections between wood framed shear walls and foundations under monotonic and cyclic load. Construction and Building Materials [Internet]. Elsevier BV; 2013 Jul;44:682–90. Available from: http://dx.doi.org/10.1016/j.conbuildmat.2013.02.055
[8] CEN 2006 EN 1995-1-1 Eurocode 5: Design of Timber structures – Part 1-1: General – Common rules and rules for buildings.
[9] Hašpl: Dílčí protokol č. 39-12208/1, Jablonec nad Nisou, ČR: SZÚ. 2015
[10] SMath Project. . [online]. 22.4.2016 [cit. 2016-04-22]. Available from: http://en.smath.info/
[11] Abaqus 6.14-1 documentation, Abaqus Analysis User's manual Simulia, 2014.
[12] Ormarsson S., Dahlblom O., Petersson H.: A numerical study of the shape stability of sawn timber subjected to moisture variation Part 2: Simulation of drying board. Wood Science and Technology [Internet]. Springer Science + Business Media, 8;33(5):407–23, 1999. Available from: http://dx.doi.org/10.1007/s002260050126.
[13] Werner H, Siebert W.: Neue Untersuchungen mit Nägeln für den Holzbau. Holz als Roh- und Werkstoff [Internet]. Springer Science + Business Media, 49(5):191–8. 1991 Available from: http://dx.doi.org/10.1007/bf02613269